Journal of Inflammation Research

Dovepress
Taylor & Francis Group

Open Access Full Text Article

ORIGINAL RESEARCH

Identification of Fatty Acid Metabolism Disorder-Related Gene Signature in Septic Cardiomyopathy

Liman Li[1–3], Tiancong Zhang[1–3], Chuan Yang[4], Qiang Meng[1–3], Shuang Wang[1–3], Yang Fu[1–3]

[1]Department of Laboratory Medicine, West China Hospital of Sichuan University, Chengdu, Sichuan Province, People's Republic of China; [2]Sichuan Clinical Research Center for Laboratory Medicine, Chengdu, Sichuan, People's Republic of China; [3]Clinical Laboratory Medicine Research Center, West China Hospital, Sichuan University, Chengdu, Sichuan, People's Republic of China; [4]Laboratory of Pulmonary Immunology and Inflammation, Frontiers Science Center for Disease-Related Molecular Network, West China Hospital of Sichuan University, Chengdu, Sichuan, People's Republic of China

Correspondence: Yang Fu, Email fuyang827@wchscu.cn

Background: Septic cardiomyopathy (SCM) is a prevalent complication of sepsis and a primary contributor to mortality in patients with sepsis. Although fatty acid metabolism (FAM) is known to regulate cardiac function, its specific role in the pathogenesis of SCM remains unclear.

Methods: The SCM datasets were obtained from the NCBI GEO database. Differentially expressed genes (DEGs) were subjected to GO and KEGG pathway analyses. The fatty acid metabolism-related genes were obtained from the MSigDB database. CytoHubba and machine learning algorithms identified hub FAM-DEGs. Associated transcriptional factors and miRNAs of hub FAM-DEGs were predicted using Cytoscape software and miRWalk 3.0 database. The immune infiltration pattern in SCM was analyzed using the ImmuCellAI tool. The relationship between hub FAM-DEGs and immune infiltration abundance was investigated using Spearman method. Hub FAM-DEGs expression levels were validated in clinical samples and mouse models.

Results: Five hub FAM-DEGs associated with SCM were identified, including *Hsd17b7, Dhcr24, Cyp1a1, Ephx1* and *Hmgcs2*. Immune analysis revealed significantly increased infiltrations of granulocytes, monocytes, M1 macrophage and neutrophils in the SCM group. Spearman analysis demonstrated that the hub FAM-DEGs were positively associated with the infiltration of pro-inflammatory immune cells. In Vivo, Down-regulations of Dhcr24 mRNA and protein levels in cardiac tissues were observed in the SCM mouse group. Clinically, the plasma concentration of DHCR24 was significantly decreased in patients with SCM.

Conclusion: This study revealed fatty acid metabolism played a crucial role in SCM and identified DHCR24 may act as a potential diagnostic biomarker and therapeutic target in SCM.

Keywords: Sepsis, septic-cardiomyopathy, fatty acid metabolism, DHCR24

Introduction

Sepsis is a leading cause of mortality in intensive care unit (ICU) patients. Global sepsis-related mortality reaches ~11 million annually, highlighting its critical impact.[1] Sepsis is characterized by an aberrant immune response to infection, which can result in organ dysfunction.[2] Among the complications of sepsis, septic cardiomyopathy (SCM) exhibits a high mortality rate and unfavorable prognosis, remaining a clinical challenge.[3] There is a lack of universal agreement on the definition of SCM, with Martin et al providing the following definition: (1) left ventricular dilation accompanied by normal or decreased filling pressure, (2) reduced ventricular contractility, and (3) right ventricular diastolic dysfunction or left ventricular [systolic and/or diastolic] dysfunction, accompanied by decreased volume responsiveness.[4] The pathological mechanisms of SCM are complex, mainly including myocardial inhibition, sympathetic nerve activation, mitochondrial damage, and calcium homeostasis imbalance.[5–7]

Received: 2 July 2024
Accepted: 8 April 2025
Published: 17 May 2025

Metabolism investigations have demonstrated that sepsis induces a notable disruption in the fatty acid metabolism.[8] In sepsis, numerous lipids, including lysophospholipids, sphingolipids, phosphatidylcholine, and chlorofatty acids, are depleted.[9] The decrease in levels of these bioactive lipids is linked to poor clinical outcomes in patients with sepsis.[10] Fatty acids play crucial roles as the predominant energy substrates for heart, providing a plethora of indispensable coenzymes necessary for mitochondrial oxidative phosphorylation.[11] The maintenance of proper cardiac function is dependent upon the regulation of fatty acid metabolism.[12] Therefore, elucidating the link between fatty acid metabolism and SCM pathogenesis is critical for identifying novel therapeutic targets.

This study explored the role of hub fatty acid metabolism-related DEGs (FAM-DEGs) inSCM. Additionally, a comprehensive regulatory network surrounding the hub FAM-DEGs in SCM was constructed. An investigation was carried out to identify the relationship between hub FAM-DEGs and immune infiltrates in SCM, with a goal of improving our understanding of the immunometabolism underlying the pathogenesis of SCM.

Materials and Methods

Data Retrieval

SCM datasets were retrieved from the NCBI GEO database (http://www.ncbi.nlm.nih.gov/geo)[13] using the search terms "septic cardiomyopathy" and "septic heart". We further screened them based on information such as animal species and entry type. Finally, the GSE142615 and GSE171546 datasets were employed in this study. The GSE142615 dataset is generated by the GPL27951 platform, containing the sequencing data for 8 cardiac tissues. Above mice cardiac tissues were collected after intraperitoneal injection of lipopolysaccharide (4 samples) or saline (4 samples).[14] The GSE171546 dataset is generated by the GPL24247 platform, and the sequencing data were composed of 15 heart tissues obtained from the septic mouse model and 5 heart tissues obtained from the controls.[15] Detailed information on the datasets is provided in Table 1.

Identification of Differentially Expressed Genes (DEGs)

Data obtainedfrom the GSE142615 and GSE171546 datasets were downloaded using R package "GEO query". DEGs were identified using R package "limma". Genes with adjusted $p < 0.05$ and $|\log2 \text{ fold change (FC)}| \geq 1$ were considered as DEGs. The DEGs were visualized by volcano plots using R package "ggplot2" and heatmaps using R package "pHeatmap".

Functional Enrichment Analysis

Gene Set Enrichment Analysis (GSEA) was conducted using R package "clusterProfiler", with the "mh.all.v2023.1.Mm.symbols.gmt" as the reference gene set, the number of permutations as 10,000. The criteria of significant results were set as normal enrichment score ($|NES| > 1$), normal $p < 0.05$, and FDR < 0.25. Gene Ontology (GO) and Kyoto Encyclopedia of Genes and Genomes (KEGG) pathway enrichment analyses for DEGs were performed using R package "clusterProfiler", and the results with $p < 0.05$ were statistically significant. The results were visualized by chordal and circle graphs using R package "ggplot2".

Identification of Fatty Acid Metabolism-Related DEGs (FAM-DEGs)

Fatty acid metabolism-related genes were obtained from the molecular signatures database (https://www.gsea-msigdb.org/gsea/index.jsp). FAM-DEGs were identified through intersecting the DEGs and the 155 fatty acid metabolism-related genes. FAM-DEGs expression patterns were visualized as heat maps using R package "ggplot2".

Table 1 Dataset Information in This Study

Dataset	Mice
GSE142615	Six hours after intraperitoneal injection of LPS (10 mg/kg) or saline solution, eight mice (LPS group, n=4; Control group, n=4) were anesthetized and the heart were collected.
GSE171546	Cardiac mRNA profiles of C57BL/6J mice after cecal ligation and puncture (CLP).

Expression and Functional Enrichment Analysis of FAM-DEGs

The expression levels of FAM-DEGs in GSE142615 and GSE171546 datasets were displayed as violin plots. Heatmaps of the correlations among FAM-DEGs were drawn using the "CorrelationPlot" plug-in in the "Origin" software. GO and KEGG pathways enrichments were performed using the "ClueGO" plug-in in the "Cytoscape" software.[16]

Hub FAM-DEGs Identification

The FAM-DEGs were processed for PPI analysis with STRING database (https://string-db.org/). Hub FAM-DEGs were identified using the CytoHubba plugin and machine learning algorithms (SVM and RF). The RF is a typical bagging ensemble algorithm, with a decision tree being the base estimator. The SVM algorithm is a powerful supervised learning algorithm, which is widely used in classification and regression problems. However, it was observed that the sample size in both the GSE142615 and GSE171546 datasets was relatively small. To address this constraint, we integrated the two datasets in machine learning applications. We employed the supplementary functionalities of the R package "sva" to mitigate the batch effects in the GSE142615 and GSE171546 datasets (Figure SI 1). Principal component analysis (PCA) was applied to evaluate the impact of batch effects. The intersected genes selected by the "CytoHubba" plug-in and the machine learning algorithms were considered as the hub FAM-DEGs.

Construction of Hub FAM-DEGs Regulatory Network

To explore the upstream regulators of hub FAM-DEGs, Transcription factors (TFs) of hub FAM-DEGs were predicted using iRegulon plug-in in the Cytoscape software.[17] The upstream miRNAs of hub FAM-DEGs were predicted using the TarBase v8.0 database (https://www.networkanalyst.ca/). The FAM-DEGs-TFs-miRNAs network was visualized using the Cytoscape software.

Immune Infiltration Analysis

The gene matrices of original datasets GSE142615 and GSE171546 were combined and normalized after elimination of the batch effect and the heterogeneity induced by different platforms with R package "sva". The normalized gene expression matrix was used for further immune infiltration analysis. The ImmuCellAI (http://bioinfo.life.hust.edu.cn/web/ImmuCellAI) estimates the infiltration abundance of 36 immune cell types based on RNA-Seq data or gene expression profiles from microarray data.[18] The normalized gene expression matrix was uploaded to the ImmuCellAI for analysis of immune infiltration, with Mann–Whitney *U*-test used for between-group comparisons. The correlation between hub FAM-DEGs and immune cells was analyzed by R package "CIBERSORT"[19]and plotted by R package "ggcorplot".

Construction of Animal Models with SCM

Our animal experiments were referenced by the study of Yingzhou Shi et al[14] . 8 to 10-week-old specific pathogen-free (SPF) grade male C57BL/6j mice were purchased from Dossy experimental animal's company. The mice were housed in an environment maintained at a temperature range of 18–22°C and a relative humidity of 50%-65%, with a controlled noise condition and a 12-hour light cycle. The stocking density was maintained at 4–5 animals per cage. The mice were provided with sterile drinking water, which was refreshed every 2 days, and approximately 50 grams of animal feed was supplied every 3–4 days. Following a 1-week acclimatization period, all mice were utilized for subsequent experimental procedures. The 6 mice were randomly divided into 2 groups receiving an intraperitoneal injection of 10 mg/kg LPS or saline solution as a control. The mice received a subcutaneous injection of sterile saline. Postoperative antibiotic treatment was not administered. The animals were subsequently placed in a temperature-controlled incubator and were monitored at 2 h intervals. About 6–7 hours after injection, all mice were killed. The myocardial pathological section and biomarkers of myocardial injury were used to confirm the success of the SCM mouse model. After dissecting the heart tissue, a portion was allocated for fixation in paraformaldehyde, while the remaining portion was processed by digesting or homogenizing the mucosal layer to facilitate RNA extraction. The welfare of experimental animals is guided by West China Hospital Guidelines for Ethical Review of Experimental Animal Welfare. All experimental manipulations were approved by the Animal Management and Use Committee of West China Hospital in Sichuan (Registration number: 20230227049).

RNA Extraction and RT–qPCR

Total RNA was extracted from the cardiac tissue and using TRIzol reagent (Invitrogen, USA) according to the manufacturer's instructions. qRT-PCR experiments were performed by Aochuang Biotechnology Co., Ltd, Chengdu, China. The primers were shown in Table SI 1.

Immunohistochemistry

IHC assays were performed by Servicebio Company (Wuhan, China). A 1:50 diluted anti-mouse Dhcr24 antibody, and a 1:200 diluted secondary antibody (Servicebio, Wuhan, China) were used for the IHC assays.

Human Study

The experimental protocol was reviewed and approved by the Medical Clinical Research Ethics Committee of West China Hospital [Registration number: 2022(868)]. A total of 30 patients with Septic cardiomyopathy were recruited from the intensive care unit (ICU) of West China Hospital between September 2023 and November 2024. We collected the blood samples of patients within 72 hours of the ICU admission. The plasma was collected to perform ELISA experiments (Ruixinbio, Quanzhou, China). All patients met the requirements according to the clinical criteria of Sepsis-3. The left ventricular ejection fraction (LVEF) of less than 50% is often considered as indicative of SCM.[20] Patients with malignancy, previous organ transplantation, HIV infection, or autoimmune diseases were not included in the study cohort. Besides, 11 age- and sex-matched healthy controls were recruited from the Physical Examination Center of West China Hospital. The baseline laboratory data were also collected.

Statistical Analysis

The data were analyzed utilizing GraphPad Prism 8.0 (GraphPad Inc, San Diego, USA). The Shapiro–Wilk test was employed to evaluate the normality of the data distribution. For data exhibiting normal distribution, the Student's *t*-test was applied, whereas nonparametric tests were employed for data that did not conform to normal distribution. A p-value of less than 0.05 was considered to indicate statistical significance.

Results

DEGs in SCM and Functional Enrichment Analysis

The flowchart illustrating data screening strategy was presented in Figure 1. Two SCM-related GEO datasets, including GSE142615 and GSE171546, were acquired for analysis. The results of the differential analysis revealed a total of 2370 DEGs in the GSE142615 dataset, with 1160 genes showing up-regulation and 1210 genes showing down-regulation in SCM samples compared to control (CON) samples. Additionally, the GSE171546 dataset exhibited 1628 DEGs, with 1139 genes up-regulated and 489 genes down-regulated. The volcano plots (Figure 2a and b) and cluster heat maps (Figure 2c and d) of DEGs were depicted respectively.

To explore the potential functions of DEGs, we performed KEGG and GSEA enrichment analysis. The results of GSEA revealed the pathways enriched with DEGs. The DEGs obtained from the GSE142615 and GSE171546 datasets were mainly involved in pathways related to cholesterol homeostasis, IFN-γ response, inflammatory response, fatty acid metabolism, coagulation and NF-kB in response to TNF-α based on |NES|>1, NOM p-val<0.05, and FDR q-val<0.25 (Figure SI 2). DEGs also underwent functional enrichment analysis usingGO andKEGG pathway analyses. The enriched GO terms were categorized into Biological Process (BP), Cellular Component (CC), and Molecular Function (MF), with notable terms including, regulation of inflammatory response, collagen-containing extracellular matrix and chemokine activity in the GSE142615 dataset. Leukocyte migration, receptor complex and cell adhesion molecule pathways were identified in the GSE171546 dataset. The enriched KEGG pathways of the DEGs in above two datasets were primarily associated with NF-kappa B signaling pathway, chemokine signaling pathway, viral protein interaction with cytokine and cytokine receptor, osteoclast differentiation, and lipid and atherosclerosis pathways (Figure 3).

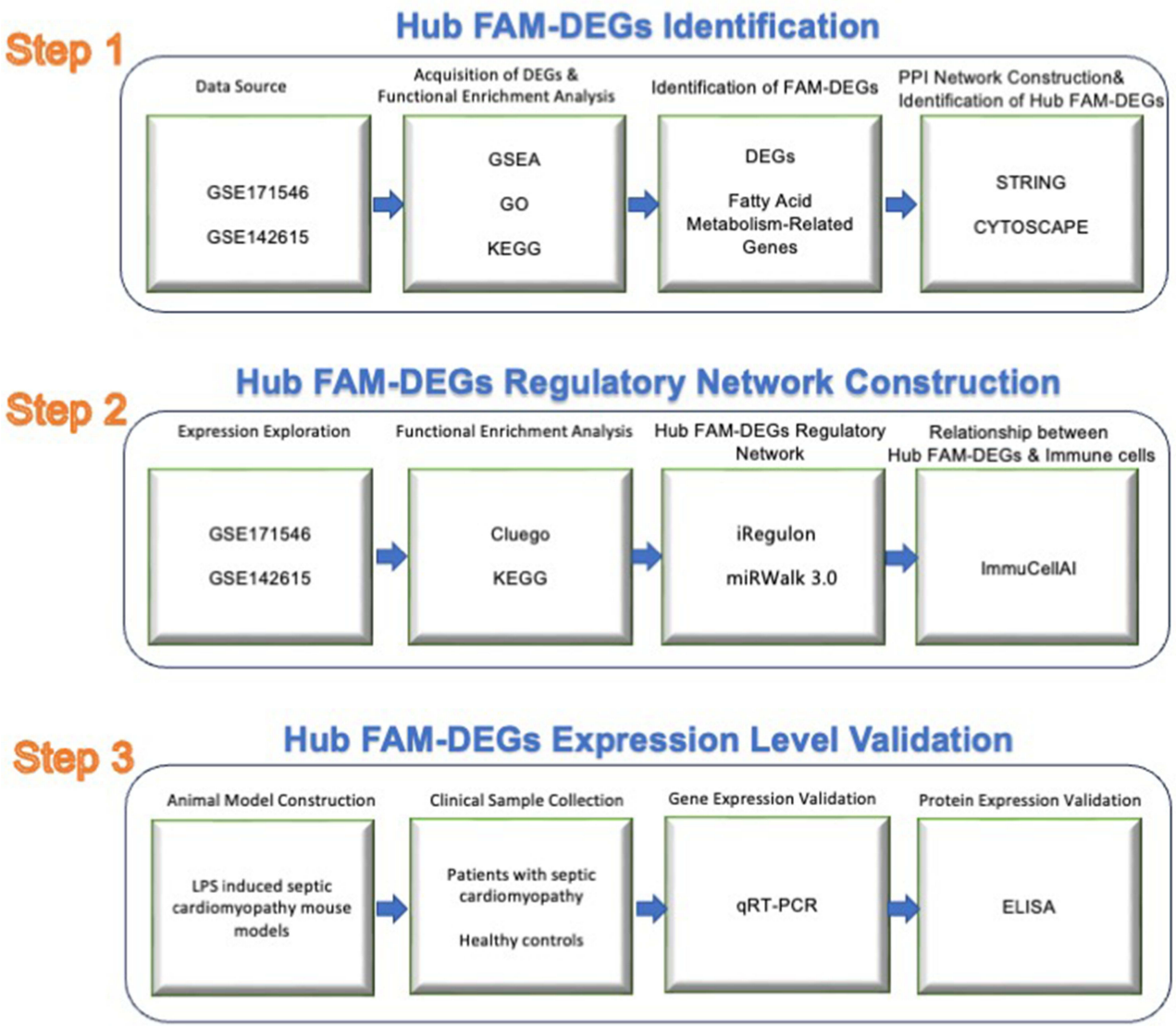

Figure 1 The flow diagram of the current study.

FAM-DEGs in SCM

Fatty acid metabolism is critical for cardiac function[21] and we aimed to explore the roles of fatty acid metabolism-related genes in SCM. The hallmark gene set of fatty acid metabolism was downloaded from MSigDB database. The genes from the intersection of fatty acid metabolism-related genes and DEGs obtained from the GSE142615 and GSE171546 datasets were considered as FAM-DEGs. We finally acquired a total of 27 FAM-DEGs (Figure 4a). There were 4 up-regulated genes and 11 down-regulated genes in the GSE142615 dataset (Figure 4b). There were 10 up-regulated genes and 5 down-regulated genes in the GSE171546 dataset (Figure 4c). The negative/positive associations between FAM-DEGs in the two datasets were also shown in two heat maps (Figure 4d and e). For example, *Aqp7, Ephx1, Ltc4s*, and *Inmt* were negatively correlated with *Glul, Vnn1, Ube2l6* and *Eno2*, and positively correlated with other FAM-DEGs in the GSE142615 dataset. *Hmgcs2, Adipor2* and *Car4* were negatively correlated with *Dhcr24, Hsph1, Eno3, Hsd17b7* and *Cyp1a1*, and positively correlated with other FAM-DEGs in the GSE171546 dataset. Then, the 27 FAM-DEGs were further analyzed for function network using the ClueGO plug-in. The results demonstrated that the 27 FAM-DEGs exhibited enrichment in biological processes such as "acyl-CoA metabolic process", "fatty acid derivative metabolic process", "ATP generation from ADP" and "monocarboxylic acid metabolic process" (Figure 4f). These FAM-DEGs

https://doi.org/10.2147/JIR.S477110

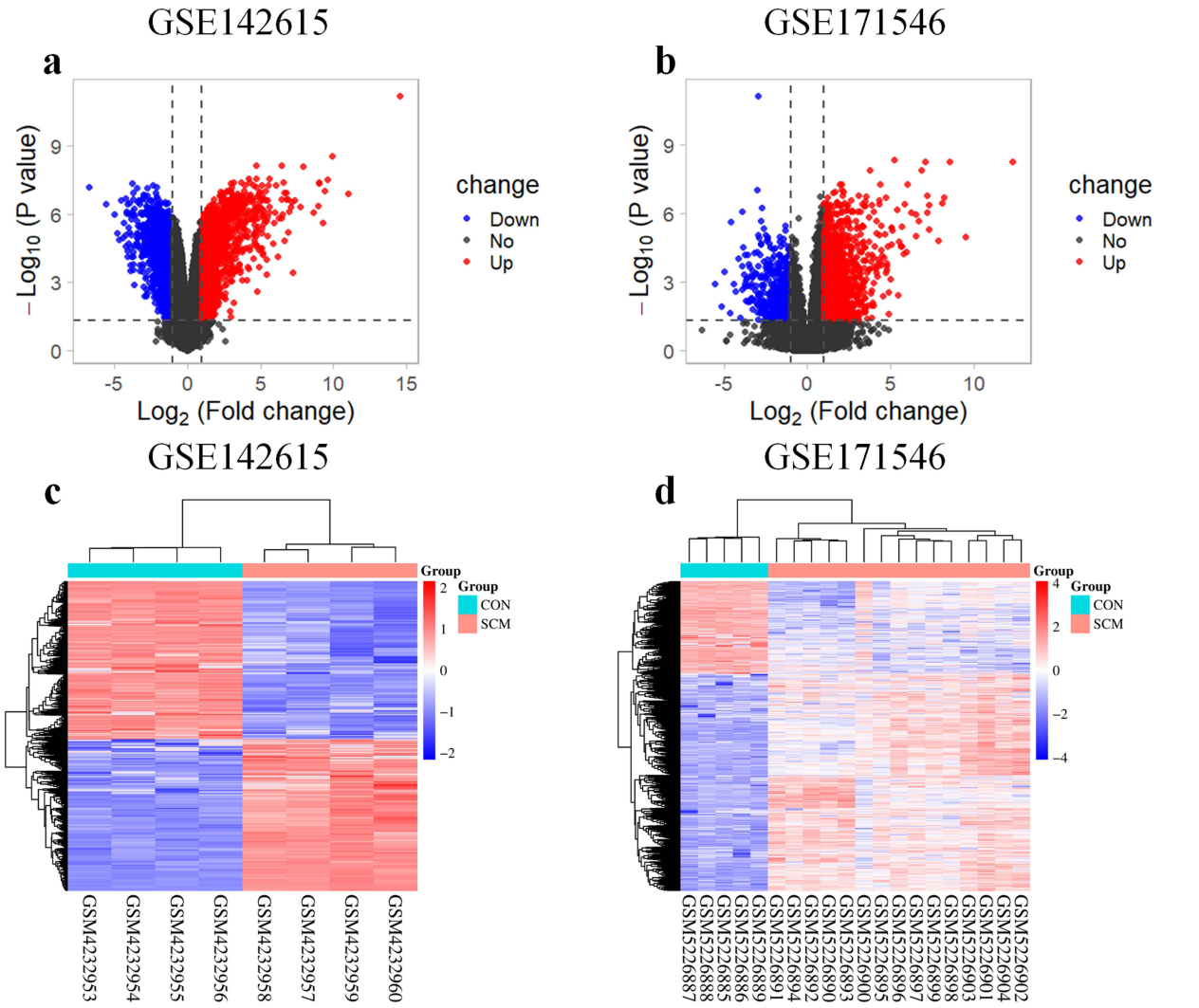

Figure 2 DEGs identification. (**a**) DEGs obtained from GSE142615 dataset were exhibited by volcano plot. (**b**) DEGs obtained from GSE171546 dataset were exhibited by volcano plot. (**c**) Heat map of GSE142615 dataset demonstrated clusters of DEGs expression levels. (**d**) Heat map of GSE171546 dataset demonstrated clusters of DEGs expression levels.

were associated with molecular functions including "hydro-lyase activity", "long chain fatty acid omega-hydroxylase activity", and "oxidoreductase activity, acting on the CH-OH group of donors, NAD or NADP as acceptor" (Figure 4g). The KEGG pathway enrichment results suggested the 27 FAM-DEGs were predominantly enriched in the pathways of "fatty acid elongation", "ovarian steroidogenesis" and "metabolism of xenobiotics by cytochrome P450" and "PPAR signaling pathway" (Figure 4h).

Hub FAM-DEGs Identification

Next, MCC algorithm of CytoHubba plug-in and machine learning algorithms were employed to screen the hub FAM-DEGs. The PPI of the 27 FAM-DEGs was analyzed using the STRING database and visualized as a network with the Cytoscape. Using the MCC algorithm within the CytoHubba plug-in, a total of 10 genes were identified as the potential candidates from the PPI network, including *Cyp4a10, Hmgcs2, Cyp1a1, Hsd17b7, Aldh3a1, Dhcr24, Fabp1, Ephx1, Adh7* and *Acot2* (Figure 5a). Results obtained from the RF algorithm exhibited that *Cyp1a1, Hsd17b7*, and *Dhcr24* were exhibited as the potential candidates among the 27 FAM-DEGs (Figure 5b). Results obtained from the SVM algorithm exhibited *Hsd17b7, Dhcr24, Ephx1*, and *Hmgcs2* may act as the potential candidates (Figure 5c). The identification of hub FAM-DEGs was achieved through the intersection of the MCC algorithm and machine learning algorithms.

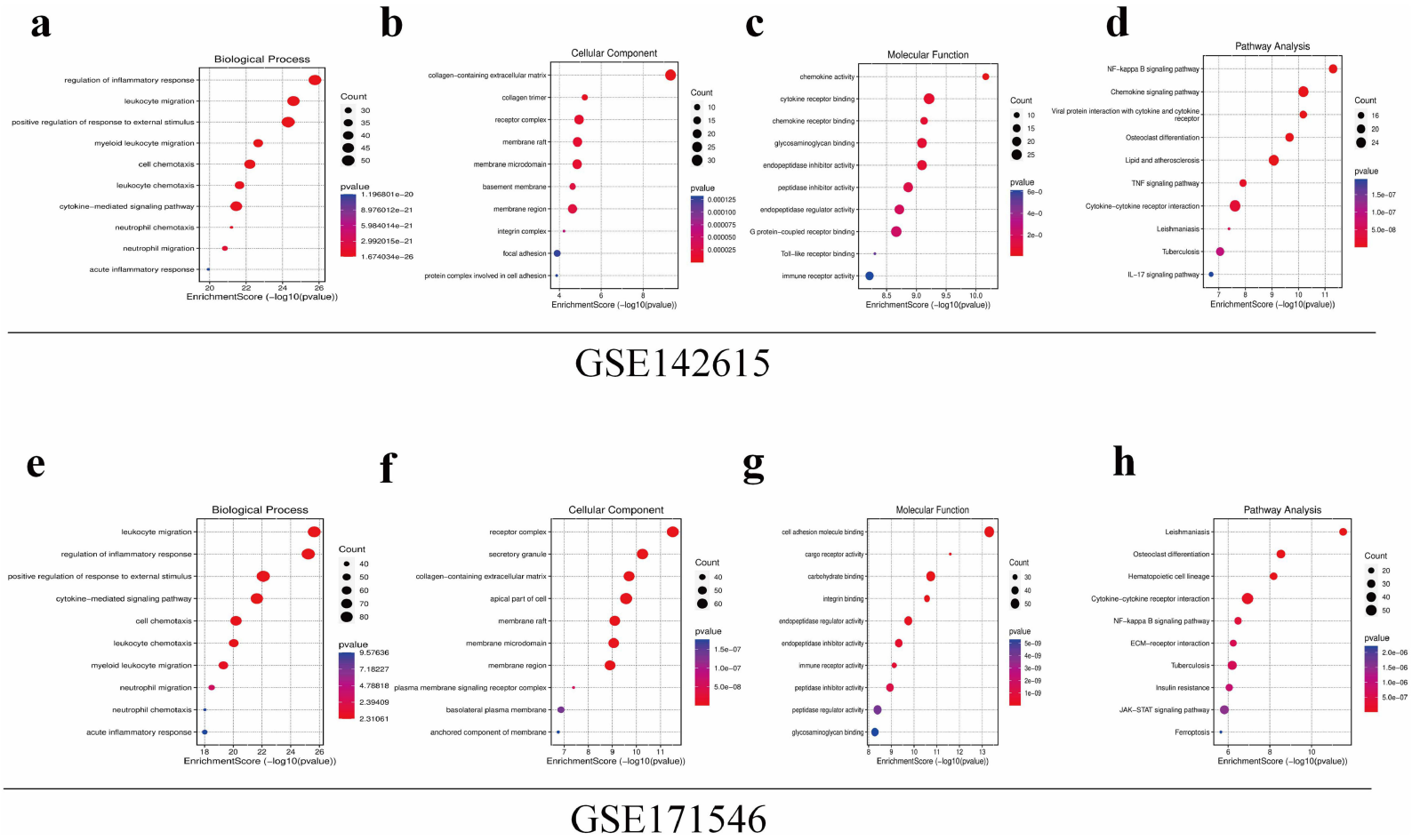

Figure 3 Functional enrichment analysis. (**a-d**) GO-BP (**a**), GO-MF (**b**), GO-CC (**c**) and KEGG (**d**) analysis of DEGs obtained from the GSE142615 dataset. (**e–h**) GO-BP (**e**), GO-MF (**f**), GO-CC (**g**) and KEGG (**h**) analysis of DEGs obtained from the GSE171546 dataset.

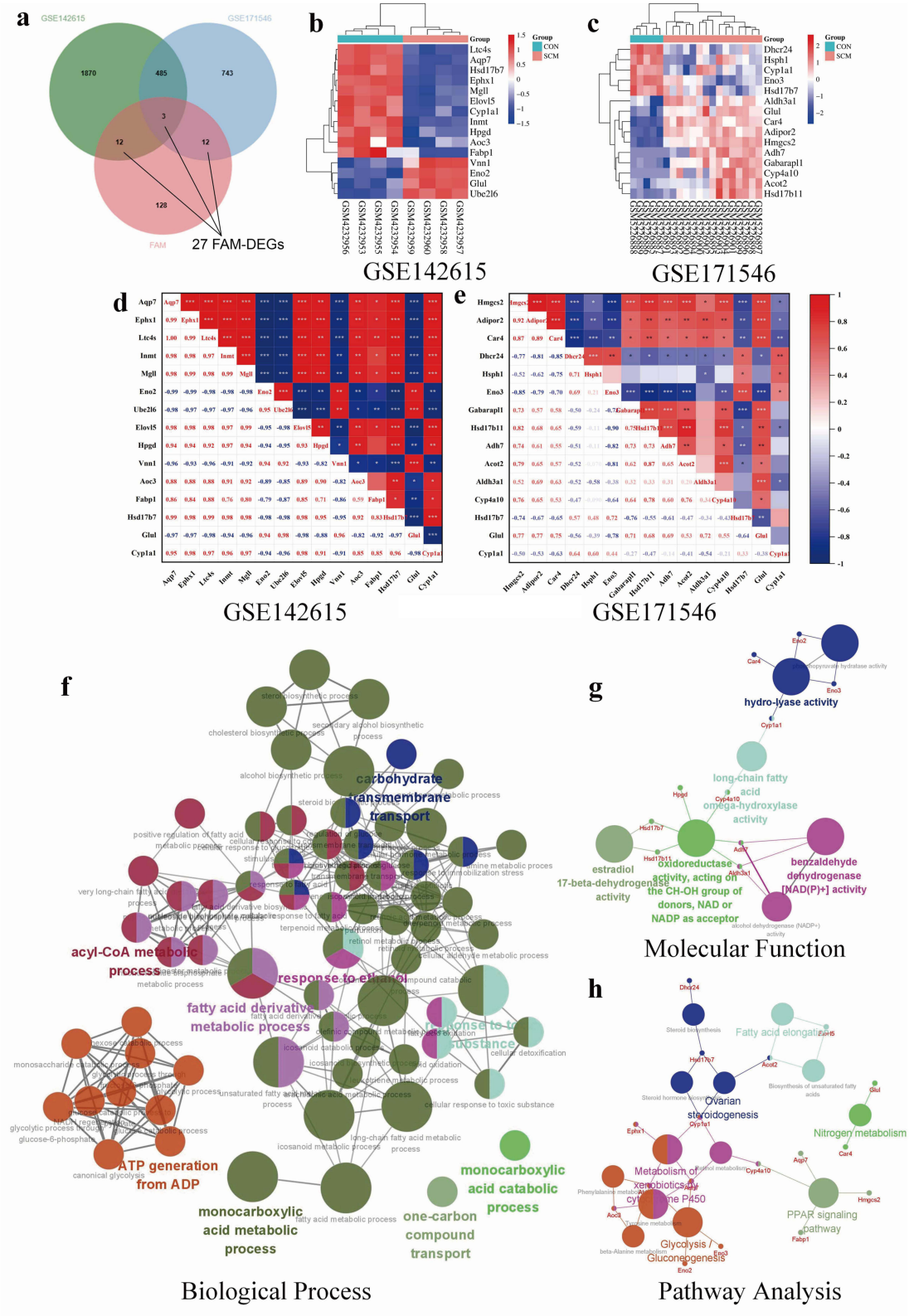

Figure 4 FAM-DEGs identification. (**a**) Intersection of DEGs and fatty acid metabolism-related genes. (**b**) Heat map of FAM-DEG expression levels in the GSE142615 dataset. (**c**) Heat map of FAM-DEG expression levels the in GSE171546 dataset. (**d**) Correlation heat map of FAM-DEGs expression levels in the GSE142615 dataset. (**e**) Correlation heat map of FAM-DEGs expression levels in the GSE171546 dataset. (**f–h**) Functional enrichment analysis of the 27 FAM-DEGs.

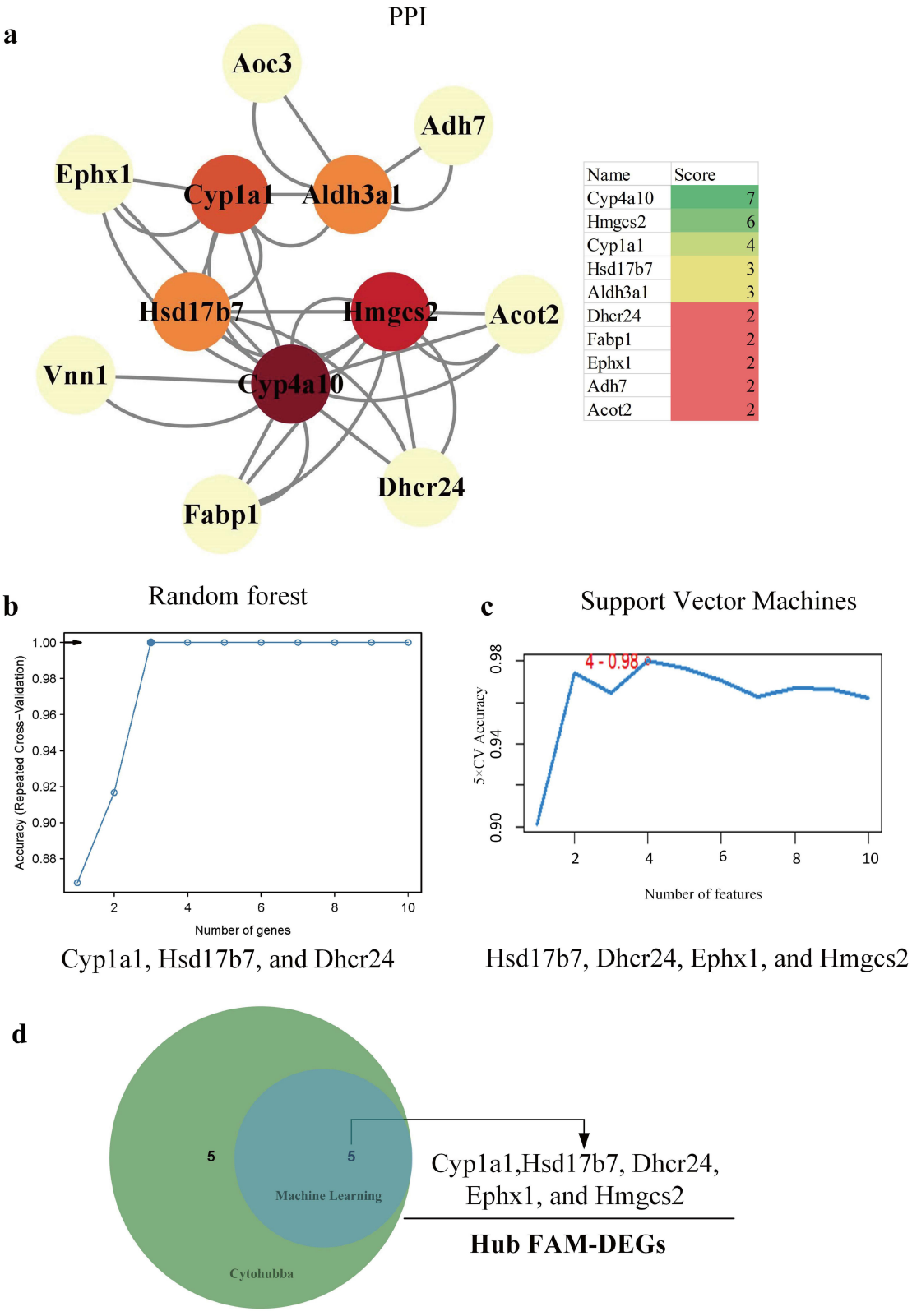

Figure 5 Hub FAM-DEGs identification. (**a**) Candidate hub FAM-DEGs identified by cytoHubba plug-in. (**b** and **c**) Candidate hub FAM-DEGs identified by machine learning algorithms. (**d**) Venn diagram showed the intersection of potential hub FAM-DEGs and 5 hub FAM-DEGs were identified.

https://doi.org/10.2147/JIR.S477110

Table 2 Names of the Hub-FAM DEGs

Gene	Full Name
Hsd17b7	Hydroxysteroid 17-Beta Dehydrogenase 7
Dhcr24	24-Dehydrocholesterol Reductase
Cyp1a1	Cytochrome P450 Family 1 Subfamily A Member 1
Ephx1	Epoxide Hydrolase 1
Hmgcs2	3-Hydroxy-3-Methylglutaryl-CoA Synthase 2

Ultimately, *Hsd17b7, Dhcr24, Cyp1a1, Ephx1*, and *Hmgcs2* were determined to be the hub FAM-DEGs (Figure 5d) and the full names of hub FAM-DEGs were shown in Table 2.

Construction of the Hub FAM-DEGs Regulatory Network

We proceeded to analyze the expression patterns of hub FAM-DEGs. The expression levels of *Cyp1a1, Ephx1*, and *Hsd17b7* were found to be down-regulated in SCM mice within the GSE142615 dataset (Figure 6a–c). In the GSE171546 dataset, the expression levels of *Cyp1a1, Dhcr24*, and *Hsd17b7* were found to be reduced, whereas the expression level of *Hmgcs2* was observed to be elevated in SCM mice (Figure 6d–g). To build the underlying hub FAM-DEGs regulatory networks, the upstream TFs and miRNAs of the hub FAM-DEGs were predicted. The upstream TFs of hub FAM-DEGs were identified using the Cytoscape software with the iRegulon plug-in. The TFs-hub FAM-DEGs regulatory network comprising 15 TFs (*Cebpa, Gabpa, Foxa1, Klf13, Glis2, Sp3, Creb3l1, Nr5a2, Mafk, Nfyb, Twist2, Nr1h4, Gm13152, Onecut2, Dus3l*) was constructed (Figure 6h). In addition, the upstream miRNAs associated with hub FAM-DEGs were predicted using the miRWalk 3.0 database, and the miRNAs-hub FAM-DEGs regulatory network was established, comprising 100 nodes and 130 edges (Figure 6I). Significantly, the mmu-mir-1a-3p, mmu-mir-155-5p, and mmu-mir-122-5p were all identified as interacting with *Dhcr24, Hsd17b7*, and *Ephx1*, whereas mmu-mir-322-5p demonstrated interactions with *Dhcr24, Hsd17b7*, and *Hmgcs2* in this network.

The Associations Between Hub FAM-DEGs and Immune Cell Infiltrations in SCM

To investigate the associations between hub FAM-DEGs expressions and immune cell enrichments in SCM, the ImmuCellAI algorithm was utilized to analyze the infiltrations of 36 immune cell types in the GSE171546 and GSE142615 datasets. Significant variations were observed in 16 immune cell types between the SCM and CON groups (Figure 7a). Specifically, granulocytes, monocytes, M1 macrophage, and neutrophils were found to be more prevalent in the SCM group, whereas B cells, T cells, $CD4^+$T cells, B1 cells, germinal center B cells, plasma cells, plasmacytoid dendritic cells (pDC), mast cells, $CD4^+$Tm, naive $CD4^+$T cells, T helper cells, and Treg cells were more abundant in the CON group (Figure 7b). Further analysis of correlations between the hub FAM-DEGs and the immune infiltrating cells showed that *Hmgcs2* was positively correlated with M1 macrophage, neutrophils, monocytes, and granulocytes, and negatively correlated with other immune cells. *Cyp1a1, Hsd17b7*, and *Dhcr24* were negatively correlated with monocytes, granulocytes, and neutrophils, and positively correlated with Treg cells, T helper cells, naive $CD4^+$T cells and B cells (Figure 7c).

Experimental Validations of Hub FAM-DEGs Expressions in Mice and Human

To ensure that the hub FAM-DEGs impacted SCM, we performed the validation experiments in animal models and clinical specimens. First, mice were utilized for creating SCM models by LPS injection (10 mg/kg) referenced by the study of Yueliang Shen[14] (Figure 8a). The myocardial pathological section and biomarkers of myocardial injury were used to confirm the success of the SCM mouse model (Figure 8b and c). The expression levels of *Hsd17b7, Dhcr24, Cyp1a1, Ephx1, and Hmgcs2* were validated in the SCM mouse models using qRT-PCR. As compared to the control group, the expressions of *Dhcr24* and *Ephx1* were significantly decreased in the SCM group, while the remaining 3 genes

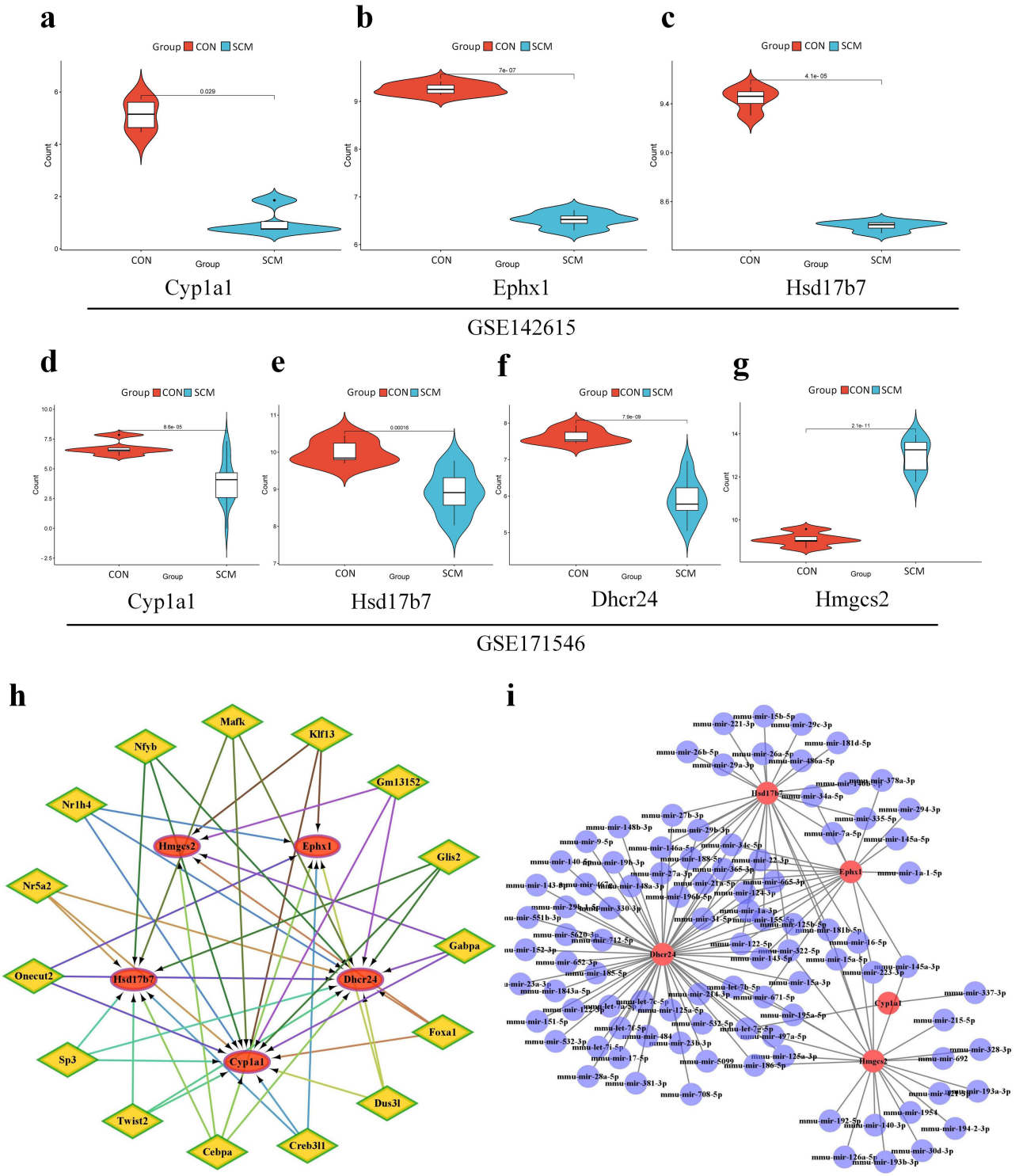

Figure 6 Construction of the hub FAM-DEGs regulatory network. (**a–c**) Expression levels of hub FAM-DEGs in the GSE142615 dataset. (d–g) Expression levels of hub FAM-DEGs in the GSE171546 dataset. (**h**) Regulatory network of hub TFs-FAM-DEGs. (**i**) Regulatory network of miRNAs -hub FAM-DEGs.

were not differentially regulated between SCM and control group or inconsistent with the results of bioinformatics analysis (Figure 8d). We further validated the protein expressions of Dhcr24 and Ephx1 between the SCM and control groups using immunohistochemistry. The results indicated that the reduced protein expression of Dhcr24 in the SCM group was consistent with its mRNA level (Figure 8c). In our clinical study, we included 11 healthy controls and 30

https://doi.org/10.2147/JIR.S477110

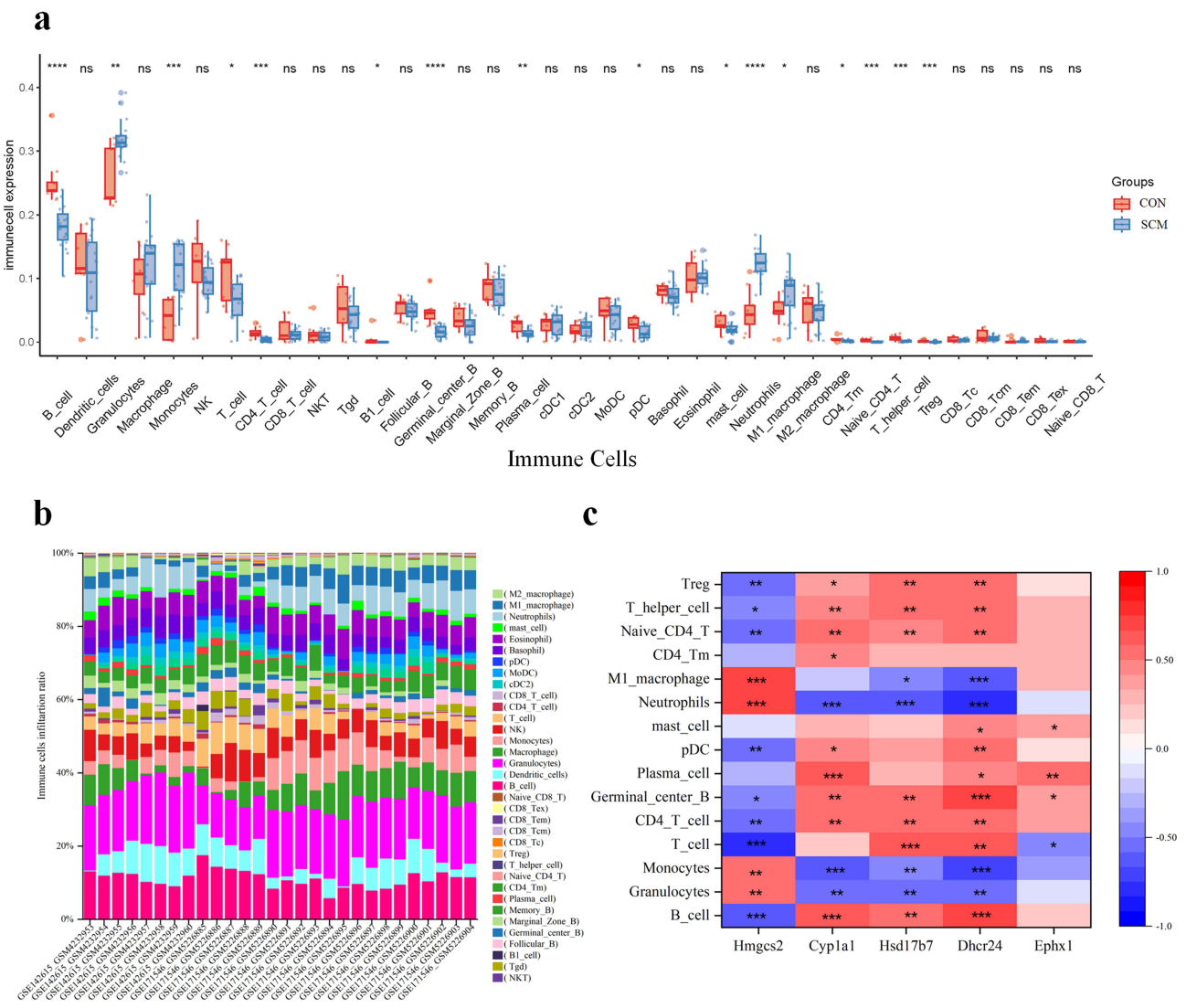

Figure 7 The associations between hub FAM-DEGs and immune cell infiltrations. (**a** and **b**) The ImmuCellAI algorithm was used to predict immune cell infiltrations in the controls and SCM groups. (**c**) The correlations of the hub FAM-DEGs with different immune cell types. *P<0.05, **P<0.01, ***P<0.001, ****P < 0.0001.

patients with septic cardiomyopathy (Table 3). We assessed the expression levels of DHCR24 in plasma using ELISA assays in both the SCM and control groups. The results indicated a significant decrease in DHCR24 concentration in patients with septic cardiomyopathy compared to the healthy controls (Figure 9a). Moreover, DHCR24 levels were significantly lower in patients experiencing septic shock compared to those without shock (Figure 9b). Additionally, we explored the correlation between DHCR24 and myocardial markers, such as lactate dehydrogenase (LDH), creatine kinase (CK), and CK-MB, within the septic cardiomyopathy cohort. The results revealed a negative correlation between DHCR24 concentration and CK-MB levels (Figures 9c–e). Collectively, these findings suggest that DHCR24 is associated with the severity of sepsis in the context of cardiomyopathy.

Discussion

The incidence of sepsis has increased globally at a concerning pace, and sepsis frequently presents with organ dysfunction, resulting in a grim prognosis.[22,23] The pathogenesis of sepsis-induced organ dysfunction remains poorly understood, and there is a lack of effective therapeutic interventions available.[24] This study aimed to enhance our understanding of the pathogenesis of SCM and identify potential therapeutic targets. Through the utilization of various bioinformatics methods, we revealed that the DEGs were significantly enriched in pathways associated with fatty acid

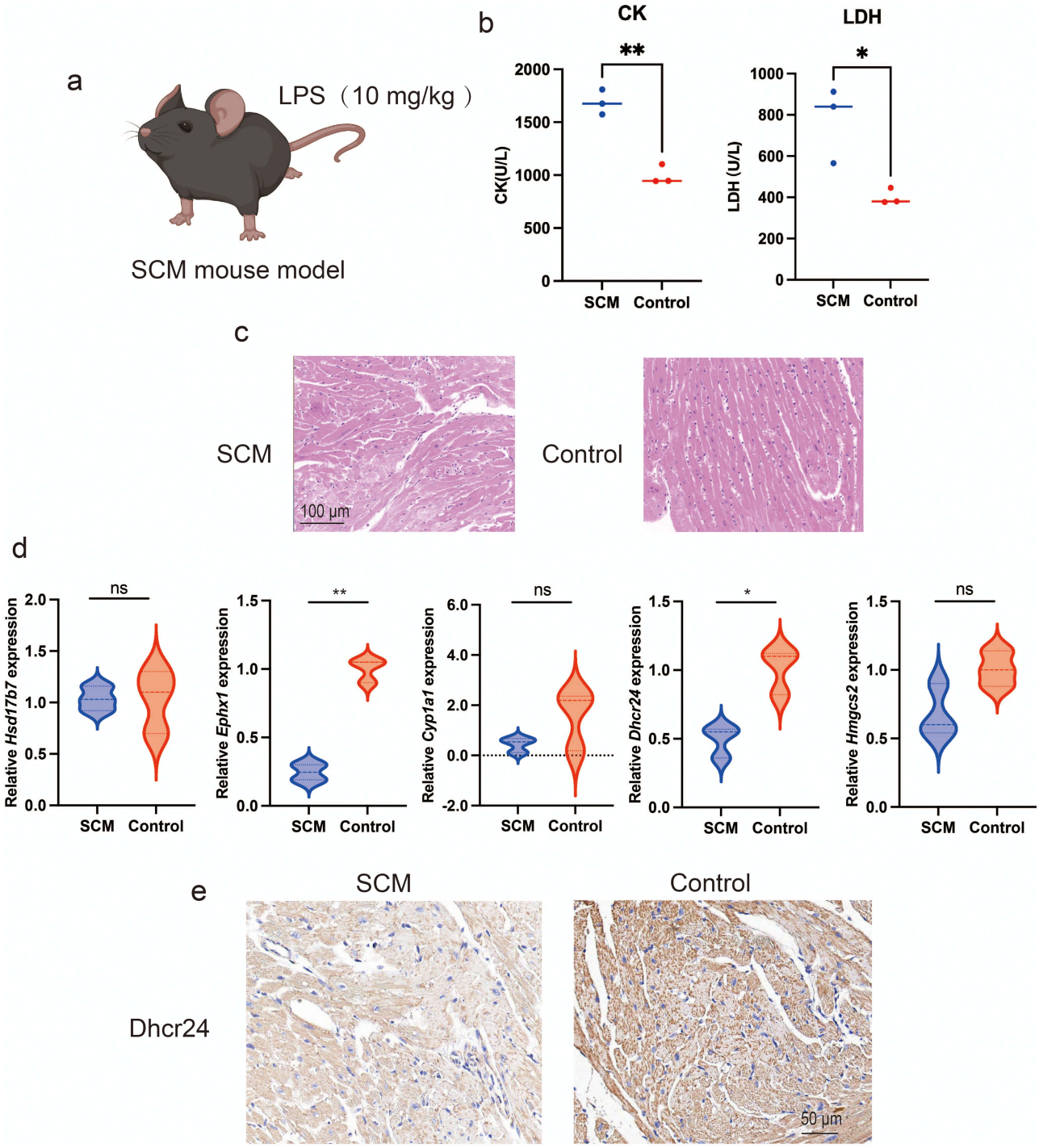

Figure 8 Validations of hub FAM-DEGs expression levels in Vivo. (**a**) SCM mouse models were induced by LPS injection (10 mg/kg). (**b** and **c**) The myocardial pathological section and biomarkers of myocardial injury were used to confirm the success of the SCM mouse model. (**d**) Hub FAM-DEGs expressions in cardiac tissues of the SCM and control groups were identified by qRT-PCR. (**e**) Immunohistochemical analysis of Dhcr24 expression in cardiac tissues of the SCM and control groups. *P<0.05, **P<0.01.

metabolism. Furthermore, we have identified the potential roles of hub-FAM-DEGs in SCM using SCM mouse models and clinical human samples.

Presently, fatty acid metabolism-related DEGs (FAM-DEGs) in SCM have not yet been reported by bioinformatics studies. This study utilized data obtained from databases to identify five hub FAM-DEGs strongly correlated with SCM,

https://doi.org/10.2147/JIR.S477110

Table 3 Clinical Characteristics of Healthy Controls and Patients with Septic Cardiomyopathy

Clinical Characteristics	Healthy Controls (n=11)	Patients with Septic Cardiomyopathy (n=30)
Male	7	21
Age, years	62.1 (52.2-65.1)	64.7 (56.7-71.7)
WBC, 10^9/L	6.5 (4.3-7.3)	9.5 (5.8-17.4)
CRP, mg/L	NA	10.1
Procalcitonin, ng/mL	NA	4.3 (0.9-29.7)
CK, U/L	NA	62.5 (20.5-403.5)
CK-MB, U/L	NA	2.2 (1.0-4.7)
LDH, IU/L	NA	276.0 (231.5-445.0)
Infection site, number of patients		
Respiratory	NA	22
Abdominal	NA	3
Vascular	NA	1
Urinary	NA	2
Other	NA	2
Clinic status		
SOFA	NA	7.0 (4.0-10.0)
Sepsis shock	NA	8
ICU days	NA	10.6 (5.8-17.0)
Distribution of pathogens		
Gram positive	NA	13
Gram negative	NA	15
Fungus	NA	1
Miscellaneous	NA	1

including *Hsd17b7, Dhcr24, Cyp1a1, Ephx1*, and *Hmgcs2*. Hsd17b7 has been shown to exert a broad spectrum of effects on amino acid, glucose, and energy metabolism. Aberrant expression of Hsd17b7 may disrupt energy supply to myocardial cells, potentially impairing myocardial contractility.[25,26] Dhcr24, a critical enzyme in cholesterol biosynthesis, cholesterol could impair heart function by promoting atherosclerosis, restricting blood supply to the heart, and inducing myocardial damage.[27] Thus, we speculated Dhcr24 may influence cardiac function by regulating cholesterol levels. Ctp1a1 is involved in the metabolism of polyunsaturated fatty acids, which have been shown to provide significant benefits for cardiac function.[28,29] Ephx1, an enzyme crucial for fatty acid metabolism, may enhance cardiac function by modulating pathways related to vascular function, inflammatory response, and lipid metabolism.[30] Hmgcs2, a key enzyme in the ketogenic pathway, catalyzes the conversion of acetyl-CoA to acetoacetyl-CoA. This reaction represents the initial step in ketogenesis, providing energy to critical tissues such as the heart, brain, and skeletal muscle.[31] Overall, changes in the expression of these metabolism-related genes may affect cardiac function in sepsis, and the mechanism is worthy of further investigation.

To validate these findings, sepsis mouse models were induced by LPS. The expression levels of the hub FAM-DEGs, including *Hsd17b7, Dhcr24, Cyp1a1, Ephx1*, and *Hmgcs2*, were assessed in the heart tissues of the SCM mouse models. *Dhcr24* exhibited consistent expression patterns as predicted by bioinformatics analysis, showing significant down-regulation in the SCM mouse models. Dhcr24 is a multifunctional enzyme that localizes to the endoplasmic reticulum and has neuroprotective and cholesterol-synthesizing activities.[32] There are numerous tissues in which Dhcr24 is expressed, including the brain, heart, lung, liver, and colon in human and mice.[33] Wei Dong et al have proposed that the compensatory expression of Dhcr24 protected against dilated cardiomyopathy through activated PI3K/Akt/HKII pathway and reduced Bax translocation.[34] These study supported the results of this experiment, suggesting Dhcr24 is a critical factor in the pathogenesis of myocardial injury induced by sepsis. Moreover, the upregulation of *Dhcr7*, a gene

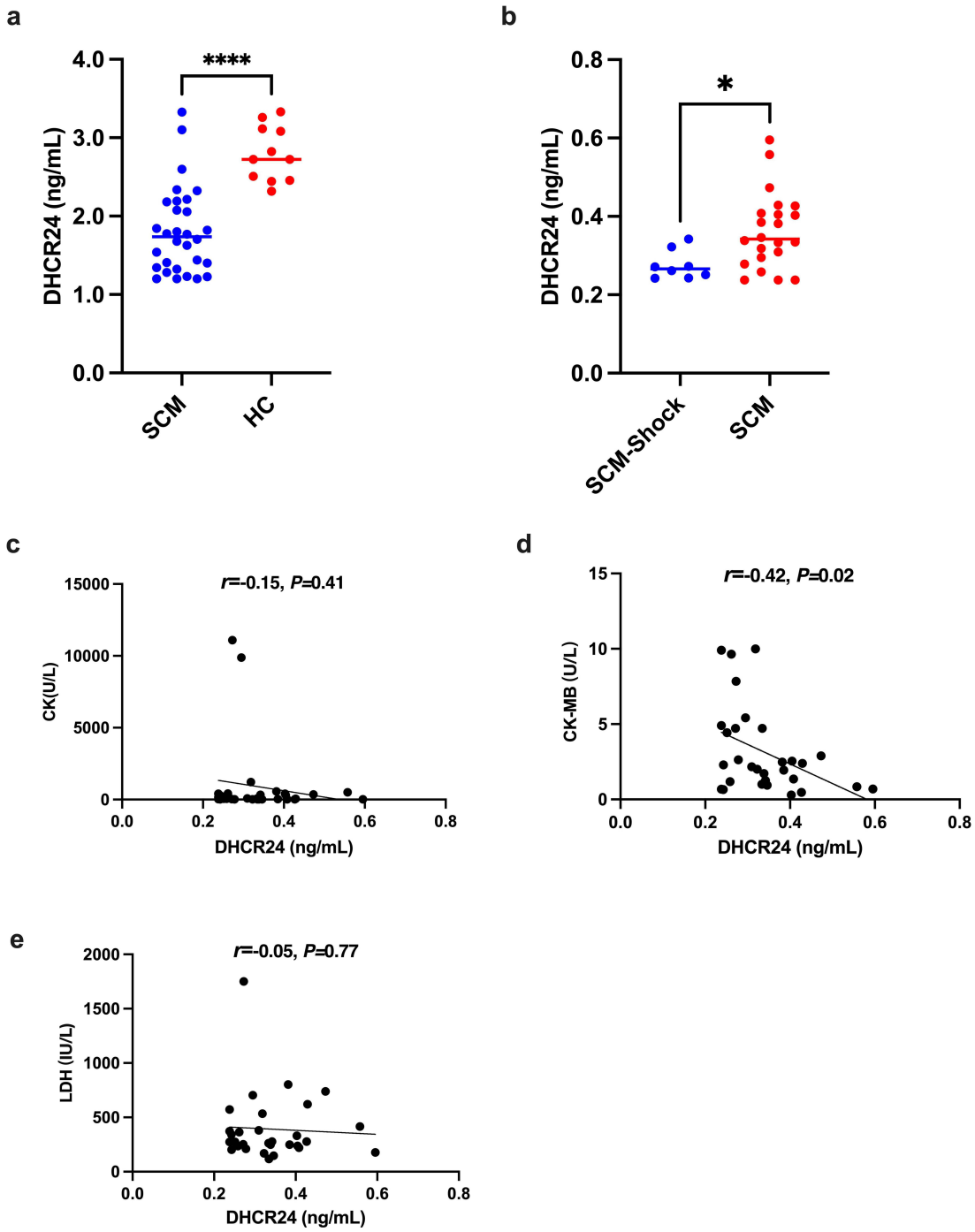

Figure 9 The change of plasma DHCR24 concentration in patients with septic cardiomyopathy. (**a**) A significant decrease in DHCR24 concentration in patients with septic cardiomyopathy compared to the healthy controls. (**b**) DHCR24 concentration was significantly lower in patients experiencing septic shock compared to those without shock. (**c**–**e**) There was a negative correlation between DHCR24 concentration and CK-MB levels, while no correlations were observed with CK or LDH levels. *P<0.05, ****P < 0.0001.

belonging to the Dhcr family, was correlated with poor outcomes in the septic zebrafish models,[35] highlighting the importance of the Dhcr family in the pathogenesis of sepsis and warranting further investigation.

Immune dysregulation is a common phenomenon in sepsis and plays a critical role in the progression of the disease.[2] We applied the ImmuCellAI to analyze immune cell infiltrations in SCM. The results showed higher enrichments of granulocytes, monocytes, M1 macrophage, and neutrophils in the SCM group than the CON group. Granulocytes could

https://doi.org/10.2147/JIR.S477110

release mediators and enzymes that potentially damage the surrounding tissue.[36] The actions of inflammatory monocytes are detrimental in acute tissue injury and contribute to infection-related mortality.[37] M1 macrophage polarization has been reported to exacerbate myocardial injury.[38] Neutrophils could enhance the ROS generation and protease release which are effectors of inflammation and tissue damage.[39] To summarize, thses cardiac immune cell infiltrations may cause excessive inflammation, leading to the occurrence of SCM. In addition, there were inverse correlations between *Dhcr24* expression and above immune cell infiltrations in SCM, suggesting *Dhcr24* may play critical roles in immunity in SCM. Further investigation will be required to elucidate the molecular mechanism involved.

We also acknowledged that several limitations were noted in the design of the current report. In this study, we identified for the first time the potential role of Dhcr24 in SCM, with its expression preliminarily validated in both clinical blood samples and animal models. Nonetheless, it is required to elucidate the mechanistic action of Dhcr24 in SCM. Further study could include in vitro studies or in vivo experiments involving Dhcr24 knockdown or overexpression in SCM mouse models. The pathophysiology of sepsis is complex, characterized by dynamic fluctuations in the immune response throughout the progression of the disease. However, our data obtained from SCM animals were analyzed at a single time point.[40] Therefore, examining the data from additional times (12, 18 and 24 hours after LPS injection) could acquire a more comprehensive understanding in SCM. Besides, the online data we used lacked relevant information about the context in which the animals live, and we did not consider the microbiome of any of the SCM mouse models. Actually, the microbiome has been demonstrated to play a crucial role in host health, with substantial evidence indicating alterations in the microbiome following the onset of sepsis.[41] Hence, future studies performing comprehensive subgroup analyses, such as polymicrobial and monomicrobial sepsis, are warranted. Moreover, to enhance the robustness of our findings and achieve a more comprehensive understanding of SCM, it is also recommended that future research integrate additional omics data, such as proteomics or metabolomics. Adopting a multi-omics approach could provide a more holistic perspective on the metabolic alterations associated with SCM, potentially uncovering novel insights into the interplay between fatty acid metabolism and cardiac dysfunction in sepsis.

Conclusion

The study underscores the involvement of fatty acid metabolism in SCM and identifies DHCR24 may act as a promising diagnostic biomarker and therapeutic target for SCM.

Abbreviation

SCM, Septic Cardiomyopathy; DEGs, Differentially Expressed Genes; FAM-DEGs, Fatty Acid Metabolism-related Differentially Expressed Genes; TFs, Transcription Factors; miRNAs, MicroRNAs; LPS, Lipopolysaccharide; LDH, Lactate Dehydrogenase; CK, Creatine Kinase; CK-MB, Creatine Kinase-MB; PCA, Principal Component Analysis; SVM, Support Vector Machine; RF, Random Forest; MCC, Maximal Clique Centrality; GSEA, Gene Set Enrichment Analysis; ImmuCellAI, Immune Cell Abundance Identifier; LVEF, Left Ventricular Ejection Fraction; ICU, Intensive Care Unit; SPF, Specific Pathogen-Free; Pdc, Plasmacytoid Dendritic Cells; Treg, Regulatory T Cells.

Data Sharing Statement

All data used to support the findings of this study are available from the corresponding author upon reasonable request.

Ethics Statement and Informed Consent

The study involving human participants was conducted in accordance with the principles outlined in the Declaration of Helsinki. Ethical approval was granted by the Medical Clinical Research Ethics Committee of West China Hospital [Registration number: 2022(868)]. Prior to participation, all individuals provided written informed consent after being thoroughly informed about the study's objectives, procedures, potential risks, and benefits, as well as their right to withdraw at any point without prejudice.

Acknowledgment

This work was financially supported by the National Natural Science Foundation of China (No. 82002215, 82402702), and the Natural Science Foundation of Sichuan Province (No. 2023NSFSC1483, 2025ZNSFSC1552).

Author Contributions

All authors made a significant contribution to the work reported, whether that is in the conception, study design, execution, acquisition of data, analysis and interpretation, or in all these areas; took part in drafting, revising or critically reviewing the article; gave final approval of the version to be published; have agreed on the journal to which the article has been submitted; and agree to be accountable for all aspects of the work.

Disclosure

The authors declare that they have no competing interests regarding the publication of this article.

References

1. Rudd KE, Johnson SC, Agesa KM, et al. Global, regional, and national sepsis incidence and mortality, 1990–2017: analysis for the Global Burden of Disease Study. *Lancet*. 2020;395(10219):200–211. doi:10.1016/S0140-6736(19)32989-7
2. Cao M, Wang G, Xie J. Immune dysregulation in sepsis: experiences, lessons and perspectives. *Cell Death Discov*. 2023;9(1):465. doi:10.1038/s41420-023-01766-7
3. Pei XB, Liu B. Research progress on the mechanism and management of septic cardiomyopathy: a comprehensive review. *Emerg Med Int*. 2023;2023:8107336. doi:10.1155/2023/8107336
4. Martin L, Derwall M, Al Zoubi S, et al. The septic heart: current understanding of molecular mechanisms and clinical implications. *Chest*. 2019;155(2):427–437. doi:10.1016/j.chest.2018.08.1037
5. Cui Y, Li Y, Meng S, et al. Molecular hydrogen attenuates sepsis-induced cardiomyopathy in mice by promoting autophagy. *BMC Anesthesiol*. 2024;24(1):72. doi:10.1186/s12871-024-02462-4
6. Lu JS. Nicorandil regulates ferroptosis and mitigates septic cardiomyopathy via TLR4/SLC7A11 signaling pathway. *Inflammation*. 2023;2023:1.
7. Xu Y, Wan W, Zeng H, et al. Exosomes and their derivatives as biomarkers and therapeutic delivery agents for cardiovascular diseases: situations and challenges. *J Transl Int Med*. 2023;11(4):341–354. doi:10.2478/jtim-2023-0124
8. Wang T, Huang Y, Zhang X, et al. Advances in metabolic reprogramming of renal tubular epithelial cells in sepsis-associated acute kidney injury. *Front Physiol*. 2024;15:1329644. doi:10.3389/fphys.2024.1329644
9. She H, Tan L, Wang Y, et al. Integrative single-cell RNA sequencing and metabolomics decipher the imbalanced lipid-metabolism in maladaptive immune responses during sepsis. *Front Immunol*. 2023;14:1181697. doi:10.3389/fimmu.2023.1181697
10. Zhou L, Li H, Hu J, et al. Plasma oxidative lipidomics reveals signatures for sepsis-associated acute kidney injury. *Clin Chim Acta*. 2023;551:117616. doi:10.1016/j.cca.2023.117616
11. Li X, Wu F, Günther S, et al. Inhibition of fatty acid oxidation enables heart regeneration in adult mice. *Nature*. 2023;622(7983):619–626. doi:10.1038/s41586-023-06585-5
12. Xu W, Billon C, Li H, et al. Novel Pan-ERR agonists ameliorate heart failure through enhancing cardiac fatty acid metabolism and mitochondrial function. *Circulation*. 2024;149(3):227–250. doi:10.1161/CIRCULATIONAHA.123.066542
13. Barrett T, Wilhite SE, Ledoux P, et al. NCBI GEO: archive for functional genomics data sets–update. *Nucleic Acids Res*. 2013;41:D991–5. doi:10.1093/nar/gks1193
14. Shi Y, Zheng X, Zheng M, et al. Identification of mitochondrial function-associated lncRNAs in septic mice myocardium. *J Cell Biochem*. 2021;122(1):53–68. doi:10.1002/jcb.29831
15. Yan X, Zhang Y-L, Han X, et al. Time series transcriptomic analysis by RNA sequencing reveals a key role of PI3K in sepsis-induced myocardial injury in mice. *Front Physiol*. 2022;13:903164. doi:10.3389/fphys.2022.903164
16. Bindea G, Mlecnik B, Hackl H, et al. ClueGO: a Cytoscape plug-in to decipher functionally grouped gene ontology and pathway annotation networks. *Bioinformatics*. 2009;25(8):1091–1093. doi:10.1093/bioinformatics/btp101
17. Janky R, Verfaillie A, Imrichová H, et al. iRegulon: from a gene list to a gene regulatory network using large motif and track collections. *PLoS Comput Biol*. 2014;10(7):e1003731. doi:10.1371/journal.pcbi.1003731
18. Miao YR, Xia M, Luo M, et al. ImmuCellAI-mouse: a tool for comprehensive prediction of mouse immune cell abundance and immune microenvironment depiction. *Bioinformatics*. 2022;38(3):785–791. doi:10.1093/bioinformatics/btab711
19. Newman AM, Liu CL, Green MR, et al. Robust enumeration of cell subsets from tissue expression profiles. *Nat Methods*. 2015;12(5):453–457. doi:10.1038/nmeth.3337
20. Song J, Yao Y, Lin S, et al. Feasibility and discriminatory value of tissue motion annular displacement in sepsis-induced cardiomyopathy: a single-center retrospective observational study. *Crit Care*. 2022;26(1):220. doi:10.1186/s13054-022-04095-w
21. O'Neill BT, Kim J, Wende AR, et al. A conserved role for phosphatidylinositol 3-kinase but not Akt signaling in mitochondrial adaptations that accompany physiological cardiac hypertrophy. *Cell Metab*. 2007;6(4):294–306. doi:10.1016/j.cmet.2007.09.001
22. Caraballo C, Jaimes F. Organ dysfunction in sepsis: an ominous trajectory from infection to death. *Yale J Biol Med*. 2019;92(4):629–640.
23. Lelubre C, Vincent JL. Mechanisms and treatment of organ failure in sepsis. *Nat Rev Nephrol*. 2018;14(7):417–427. doi:10.1038/s41581-018-0005-7
24. Nong Y, Wei X, Yu D. Inflammatory mechanisms and intervention strategies for sepsis-induced myocardial dysfunction. *Immun Inflamm Dis*. 2023;11(5):e860. doi:10.1002/iid3.860

25. He XY, Yang SY. Roles of type 10 17beta-hydroxysteroid dehydrogenase in intracrinology and metabolism of isoleucine and fatty acids. *Endocr Metab Immune Disord Drug Targets*. 2006;6(1):95–102. doi:10.2174/187153006776056639
26. Sikder K, Shukla S, Patel N, et al. High fat diet upregulates fatty acid oxidation and ketogenesis via intervention of PPAR-gamma. *Cell Physiol Biochem*. 2018;48(3):1317–1331. doi:10.1159/000492091
27. Gordts SC, Van Craeyveld E, Muthuramu I, et al. Lipid lowering and HDL raising gene transfer increase endothelial progenitor cells, enhance myocardial vascularity, and improve diastolic function. *PLoS One*. 2012;7(10):e46849. doi:10.1371/journal.pone.0046849
28. Conway DE, Sakurai Y, Weiss D, et al. Expression of CYP1A1 and CYP1B1 in human endothelial cells: regulation by fluid shear stress. *Cardiovasc Res*. 2009;81(4):669–677. doi:10.1093/cvr/cvn360
29. Huang CF, Wang W-N, Sun -C-C, et al. Echinocystic acid ameliorates hyperhomocysteinemia-induced vascular endothelial cell injury through regulating NF-kappaB and CYP1A1. *Exp Ther Med*. 2017;14(5):4174–4180. doi:10.3892/etm.2017.5097
30. Zhou Z, Zhang M, Zhao C, et al. Epoxyeicosatrienoic acids prevent cardiac dysfunction in viral myocarditis via interferon type I signaling. *Circ Res*. 2023;133(9):772–788. doi:10.1161/CIRCRESAHA.123.322619
31. Asif S, Kim RY, Fatica T, et al. Hmgcs2-mediated ketogenesis modulates high-fat diet-induced hepatosteatosis. *Mol Metab*. 2022;61:101494. doi:10.1016/j.molmet.2022.101494
32. Crameri A, Biondi E, Kuehnle K, et al. The role of seladin-1/DHCR24 in cholesterol biosynthesis, APP processing and abeta generation in vivo. *EMBO J*. 2006;25(2):432–443. doi:10.1038/sj.emboj.7600938
33. Lu X, Jia D, Zhao C, et al. Recombinant adenovirus-mediated overexpression of 3β-hydroxysteroid-Δ24 reductase. *Neural Regen Res*. 2014;9(5):504–512. doi:10.4103/1673-5374.130074
34. Dong W, Guan -F-F, Zhang X, et al. Dhcr24 activates the PI 3K/Akt/ HKII pathway and protects against dilated cardiomyopathy in mice. *Animal Model Exp Med*. 2018;1(1):40–52. doi:10.1002/ame2.12007
35. Guirgis FW, Jacob V, Wu D, et al. DHCR7 expression predicts poor outcomes and mortality from sepsis. *Crit Care Explor*. 2023;5(6):e0929. doi:10.1097/CCE.0000000000000929
36. Emal D, Rampanelli E, Stroo I, et al. Depletion of gut microbiota protects against renal ischemia-reperfusion injury. *J Am Soc Nephrol*. 2017;28(5):1450–1461. doi:10.1681/ASN.2016030255
37. Iriguchi S, Kikuchi N, Kaneko S, et al. T-cell-restricted T-bet overexpression induces aberrant hematopoiesis of myeloid cells and impairs function of macrophages in the lung. *Blood*. 2015;125(2):370–382. doi:10.1182/blood-2014-05-575225
38. Liu X, Zhang W, Luo J, et al. TRIM21 deficiency protects against atrial inflammation and remodeling post myocardial infarction by attenuating oxidative stress. *Redox Biol*. 2023;62:102679. doi:10.1016/j.redox.2023.102679
39. Chen PJ, Ko I-L, Lee C-L, et al. Targeting allosteric site of AKT by 5,7-dimethoxy-1,4-phenanthrenequinone suppresses neutrophilic inflammation. *EBioMedicine*. 2019;40:528–540. doi:10.1016/j.ebiom.2019.01.043
40. Segura-Cervantes E, Mancilla-Ramírez J, González-Canudas J, et al. Inflammatory response in preterm and very preterm newborns with sepsis. *Mediators Inflamm*. 2016;2016:6740827. doi:10.1155/2016/6740827
41. Alverdy JC, Chang EB. The re-emerging role of the intestinal microflora in critical illness and inflammation: why the gut hypothesis of sepsis syndrome will not go away. *J Leukoc Biol*. 2008;83(3):461–466. doi:10.1189/jlb.0607372